

# Cosmological model-independent test of two-point diagnostic by the observational Hubble parameter data

Shu-Lei Cao<sup>2</sup>, Xiao-Wei Duan<sup>3</sup>, Xiao-Lei Meng<sup>2</sup>, Tong-Jie Zhang<sup>a,1,2</sup>

<sup>1</sup>Dezhou University, Dezhou 253023, China

<sup>2</sup>Department of Astronomy, Beijing Normal University, Beijing, 100875, China

<sup>3</sup>Department of Astronomy, School of Physics, Peking University, Beijing 100871, China

Received: date / Accepted: date

**Abstract** Aiming at exploring the nature of dark energy (DE), we use forty-three observational Hubble parameter data (OHD) in the redshift range  $0 < z \leq 2.36$  to make a cosmological model-independent test of the two-point  $Om h^2(z_2; z_1)$  diagnostic. In  $\Lambda$ CDM model, with equation of state (EoS)  $w = -1$ ,  $Om h^2 \equiv \Omega_m h^2$  is tenable, where  $\Omega_m$  is the matter density parameter, and  $h$  is Hubble parameter at present. We utilize two methods: the weighted mean and median statistics to bin the OHD to increase the signal-to-noise ratio of the measurements. The binning methods turn out to be promising and considered to be robust. By applying the  $Om h^2(z_2; z_1)$  diagnostic to the binned data, we find that although the best-fit values of  $Om h^2$  are fluctuated as the consistent redshift intervals change, in average, they are consistent with being constant within  $1\sigma$  confidence region. Therefore, we conclude that the  $\Lambda$ CDM model cannot be ruled out.

## 1 Introduction

Over the past few decades, there have been a number of approaches proposed to quantitatively investigate the expansion history and structure growth of the universe [see 1, 2, for recent reviews]. The observations of Type Ia supernovae (SNIa) [3, 4] have provided ample evidence for an accelerating expansion to an increasing precision [5]. Other complementary probes is also strongly supportive for that phenomenon, including the baryon acoustic oscillation (BAO) measurements [6], the weak gravitational lensing [7], the abundance of galaxy clusters [8], the cosmic microwave background (CMB) anisotropies [9], the linear growth of large-scale structure [10], and the Hubble constant  $H_0$  [11]. There are plenty of cosmological models raised to account for the

acceleration phenomenon, yet the best-fit one is still uncertain.

The existence of dark energy (DE) with negative equation of state (EoS) parameter  $w \equiv p_{\text{DE}}/\rho_{\text{DE}}$  is considered as a prevailing interpretation currently. In this context, the most popular DE model being used remains to be the simple cosmological constant cold dark matter ( $\Lambda$ CDM) model, with  $w = -1$  at all times [12]. However, the popularity of  $\Lambda$ CDM model does not cover the issue that it suffers from the fine tuning and coincidence problems [13, 14]. In addition, it is worth noticing about the possibility of DE with evolving EoS [15], i.e. the dynamical DE models ( $w = w(z)$ ), such as Quintessence [ $w > -1$ , 16, 17], Phantom [ $w < -1$ , 18], K-essence [ $w > -1$  or  $w < -1$ , 19, 20], and especially Quintom [ $w$  crossing -1, 21, 22] models. Nevertheless, it deserves more profound, physical explanations for all these models. Moreover, Zhao et al. [15] find that an evolving DE can relieve the tensions presented among existing datasets within the  $\Lambda$ CDM framework. Meanwhile, it is useful to introduce diagnostics based upon direct observations and capable of revealing dynamical features of DE. One of these diagnostics is  $Om(z)$ , which is defined as a function of redshift  $z$  [23, 24], i.e.,

$$Om(z) = \frac{\tilde{h}^2(z) - 1}{(1+z)^3 - 1}, \quad (1)$$

with  $\tilde{h} = \frac{H(z)}{H_0}$  and  $H(z)$  denoting the Hubble expansion rate.  $Om(z)$  has the property of being  $\Omega_m$  for  $w = -1$  case. Moreover, Shafieloo et al. [25] modified this diagnostic to accommodate two-point situations as follows,

$$Om(z_2; z_1) = \frac{\tilde{h}^2(z_2) - \tilde{h}^2(z_1)}{(1+z_2)^3 - (1+z_1)^3}. \quad (2)$$

In this case, if  $Om(z_2; z_1) \equiv \Omega_m$  held for any redshift intervals, it would substantiate the validity of  $\Lambda$ CDM model. In

<sup>a</sup>e-mail: tjhang@bnu.edu.cn

other words, the measurements of  $Om(z_2; z_1) \neq \Omega_m$  would imply a deviation from  $\Lambda$ CDM and the fact that other DE models with an evolving EoS should be taken into account.

In this paper, we first introduce the measurements of the observational  $H(z)$  data (OHD) and then exhibit the currently available data sets in Section 2. In Section 3, we apply two binning methods: the weighted mean and median statistics techniques to OHD, and obtain the binned OHD categorically. In Section 4, based on the binned OHD, we test the  $\Lambda$ CDM model with two-point  $Om h^2(z_2; z_1)$  diagnostic. Finally, we summarize our conclusions in Section 5.

## 2 The observational $H(z)$ data sets

The OHD can be used to constrain cosmological parameters because they are obtained from model-independent direct observations. Until now, three methods have been developed to measure OHD: cosmic chronometer, radial BAO size methods [26], and gravitational wave [27]. Jimenez et al. [28] first proposed that relative galaxy ages can be used to obtain  $H(z)$  values and they reported one  $H(z)$  measurement at  $z \sim 0.1$  in their later work [29]. Simon et al. [30] added additional eight  $H(z)$  points in the redshift range between 0.17 and 1.75 from differential ages of passively evolving galaxies, and further constrained the redshift dependence of the DE potential by reconstructing it as a function of redshift. Later, Stern et al. [31] provided two new determinations from red-envelope galaxies and then constrained cosmological parameters including curvature through the joint analysis of CMB data. Furthermore, Moresco et al. [32] obtained eight new measurements of  $H(z)$  from the differential spectroscopic evolution of early-type, massive, red elliptical galaxies which can be used as standard cosmic chronometers. By applying the galaxy differential age method to SDSS DR7, Zhang et al. [33] expanded the  $H(z)$  data sample by four new points. Taking advantage of near-infrared spectroscopy of high redshift galaxies, Moresco et al. [34] obtained two measurements of  $H(z)$ . Later, they gained four more latest  $H(z)$  values [35]. Recently, Ratsimbazafy et al. [36] provides one more measurement of  $H(z)$  based on analysis of high quality spectra of Luminous Red Galaxies (LRGs) obtained with the Southern African Large Telescope (SALT).

On the other side,  $H(z)$  can also be extracted from the detection of radial BAO features. Gaztañaga et al. [37] first obtained two  $H(z)$  data points using the BAO peak position as a standard ruler in the radial direction. Blake et al. [38] further combined the measurements of BAO peaks and the Alcock-Paczynski distortion to find three other  $H(z)$  results. Samushia et al. [39] provided a  $H(z)$  point at  $z = 0.57$  from the BOSS DR9 CMASS sample. Xu et al. [40] used the BAO signals from the SDSS DR7 luminous red galaxy sample to derive another observational  $H(z)$  measurement. The  $H(z)$

value determined based upon BAO features in the Lyman- $\alpha$  forest of SDSS-III quasars was presented by Delubac et al. [41], which is the farthest precisely observed  $H(z)$  results so far. Alam et al. [42] obtained three  $H(z)$  measurements with cosmological analysis of the DR12 galaxy sample.

Moreover, Liu et al. [27] present a new method of measuring Hubble parameter by using the anisotropy of luminosity distance, and the analysis of gravitational wave of neutron star binary system.

After evaluating these data points from [43, 44], we combine these 43 OHD and present them in Table 1 and mark them in Figure 1. Note that it is obvious that the cosmic chronometer method is completely model-independent, and one may misjudge the radial BAO method to be model-dependent since they involve in some fiducial  $\Lambda$ CDM models. However, in fact, the fiducial models can not affect the results as mentioned in the references (e.g., see P. 5 of Alam et al. [42]). Moreover, the three  $H(z)$  measurements taken from Blake et al. [38] are correlated with each other, and also, the three measurements of Alam et al. [42] are correlated. This fact will affect the choice of binning range afterwards.

We use a  $\Lambda$ CDM model with no curvature term to compare theoretical values of Hubble parameter with the OHD results, with the Hubble parameter given by

$$H(z) = H_0 \sqrt{\Omega_m (1+z)^3 + 1 - \Omega_m}, \quad (3)$$

where cosmological parameters take values from the Planck temperature power spectrum measurements [9]. The best fit value of  $H_0$  is  $67.81 \text{ km s}^{-1} \text{ Mpc}^{-1}$ , and  $\Omega_m$  is 0.308. The theoretical computation of  $H(z)$  based upon this  $\Lambda$ CDM is also shown in Figure 1.

Being independent observational data,  $H(z)$  determinations have been frequently used in cosmological research. One of the leading purposes is using them to constrain DE. Jimenez & Loeb [28] first proposed that  $H(z)$  measurements can be used to constrain DE EoS at high redshifts. Simon et al. [30] derived constraints on DE potential using  $H(z)$  results and supernova data. Samushia & Ratra [45] began applying these measurements to constraining cosmological parameters in various DE models. In the meanwhile, DE evolution came into its own as an active research field in the last twenty years [46–50]. To sum up, the OHD are proved to be very promising towards understanding the nature of DE.

In the next section, we will bin the OHD in Table 1 by using two binning techniques.

## 3 Binning OHD

As stated by Farooq et al. [44, 51], there are two techniques: the weighted mean and median statistics, which can be used to bin Hubble parameter measurements. In [44], they listed two reasons to compute “average”  $H(z)$  values for bins in

$z$	$H(z)$	Method	Ref.
0.0708	$69.0 \pm 19.68$	I	Zhang et al. (2014)
0.09	$69.0 \pm 12.0$	I	Jimenez et al. (2003)
0.12	$68.6 \pm 26.2$	I	Zhang et al. (2014)
0.17	$83.0 \pm 8.0$	I	Simon et al. (2005)
0.179	$75.0 \pm 4.0$	I	Moresco et al. (2012)
0.199	$75.0 \pm 5.0$	I	Moresco et al. (2012)
0.2	$72.9 \pm 29.6$	I	Zhang et al. (2014)
0.240	$79.69 \pm 2.65$	II	Gaztañaga et al. (2009)
0.27	$77.0 \pm 14.0$	I	Simon et al. (2005)
0.28	$88.8 \pm 36.6$	I	Zhang et al. (2014)
0.35	$84.4 \pm 7.0$	II	Xu et al. (2013)
0.352	$83.0 \pm 14.0$	I	Moresco et al. (2012)
0.38	$81.5 \pm 1.9$	II	Alam et al. (2016)
0.3802	$83.0 \pm 13.5$	I	Moresco et al. (2016)
0.4	$95 \pm 17.0$	I	Simon et al. (2005)
0.4004	$77.0 \pm 10.2$	I	Moresco et al. (2016)
0.4247	$87.1 \pm 11.2$	I	Moresco et al. (2016)
0.43	$86.45 \pm 3.68$	II	Gaztañaga et al. (2009)
0.44	$82.6 \pm 7.8$	II	Blake et al. (2012)
0.4497	$92.8 \pm 12.9$	I	Moresco et al. (2016)
0.47	$89 \pm 67$	I	Ratsimbazafy et al. (2017)
0.4783	$80.9 \pm 9.0$	I	Moresco et al. (2016)
0.48	$97.0 \pm 62.0$	I	Stern et al. (2010)
0.51	$90.4 \pm 1.9$	II	Alam et al. (2016)
0.57	$92.4 \pm 4.5$	II	Samushia et al. (2013)
0.593	$104.0 \pm 13.0$	I	Moresco et al. (2012)
0.6	$87.9 \pm 6.1$	II	Blake et al. (2012)
0.61	$97.3 \pm 2.1$	II	Alam et al. (2016)
0.68	$92.0 \pm 8.0$	I	Moresco et al. (2012)
0.73	$97.3 \pm 7.0$	II	Blake et al. (2012)
0.781	$105.0 \pm 12.0$	I	Moresco et al. (2012)
0.875	$125.0 \pm 17.0$	I	Moresco et al. (2012)
0.88	$90.0 \pm 40.0$	I	Stern et al. (2010)
0.9	$117.0 \pm 23.0$	I	Simon et al. (2005)
1.037	$154.0 \pm 20.0$	I	Moresco et al. (2012)
1.3	$168.0 \pm 17.0$	I	Simon et al. (2005)
1.363	$160.0 \pm 33.6$	I	Moresco (2015)
1.43	$177.0 \pm 18.0$	I	Simon et al. (2005)
1.53	$140.0 \pm 14.0$	I	Simon et al. (2005)
1.75	$202.0 \pm 40.0$	I	Simon et al. (2005)
1.965	$186.5 \pm 50.4$	I	Moresco (2015)
2.34	$222.0 \pm 7.0$	II	Delubac et al. (2015)
2.36	$226.0 \pm 8.0$	II	Font-Ribera et al. (2014)

Table 1: The current available OHD dataset. Where I and II represent the cosmic chronometer and the radial BAO method, respectively, and  $H(z)$  is in units of  $\text{km s}^{-1} \text{Mpc}^{-1}$  here.

redshift space. On the one hand, the weighted mean technique can indicate whether the original data have error bars inconsistent with Gaussianity. On the other hand, the binned data can more clearly visually illustrate tendencies as a function of redshift, without the assumption of a particular cosmological model.

As for the weighted mean technique, the ideal choice should be a trade-off between bin size and number of measurements per bin that maximizes both quantities. In order to avoid correlations at one bin, we choose 3-4, 4-5, 5-6, and 5-6-7 measurements per bin, which separates the correlated

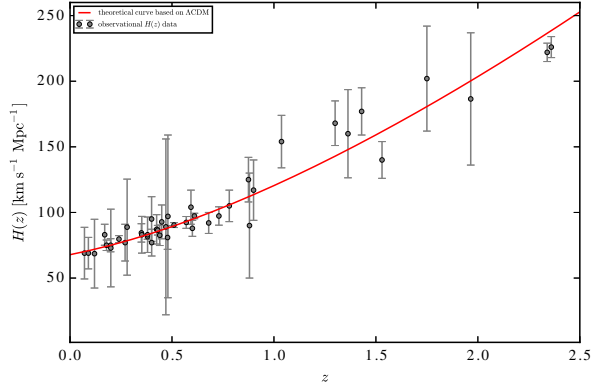


Fig. 1: The full OHD set and theoretical curve of standard flat  $\Lambda$ CDM model. The OHD are represented by gray points along with the uncertainties. The red curve shows theoretical  $H(z)$  evolution based upon the adopted  $\Lambda$ CDM model which is described in Section 2.

data, and the last four measurements are binned by twos for all the cases.

According to Podariu et al. [52], the weighted mean of  $H(z)$  is given by

$$\bar{H}(z) = \frac{\sum_{i=1}^N (H(z_i)/\sigma_i^2)}{\sum_{i=1}^N 1/\sigma_i^2}, \quad (4)$$

where  $H(z_i)$  and  $\sigma_i$  stand for the Hubble parameter data and one standard deviation for  $i = 1, 2, \dots, N$  measurements in the binning redshift range. Similarly, the corresponding weighted bin redshift  $\bar{z}$  and weighted error  $\bar{\sigma}$  are as follows,

$$\bar{z} = \frac{\sum_{i=1}^N (z_i/\sigma_i^2)}{\sum_{i=1}^N 1/\sigma_i^2}, \quad (5)$$

and

$$\bar{\sigma} = \sqrt{\frac{1}{\sum_{i=1}^N 1/\sigma_i^2}}. \quad (6)$$

The goodness of fit for each bin, the reduced  $\chi^2_v$ , can be expressed as

$$\chi^2_v = \frac{1}{N-1} \sum_{i=1}^N \frac{(H(z_i) - \bar{H}(z))^2}{\sigma_i^2}. \quad (7)$$

The number of standard deviations which  $\chi^2_v$  deviates from the expected value is presented as

$$N_\sigma = |\chi_v - 1| \sqrt{2(N-1)}. \quad (8)$$

Non-Gaussian measurements, the presence of unaccounted-for systematic errors, or correlations between measurements can result in large  $N_\sigma$ . The weighted mean results for the binned  $H(z)$  measurements are listed in Table 2, where the  $N_\sigma$  values are considerably small for all bins, just like results of Farooq et al. [44], hence indicating that the 43 OHD are not inconsistent with Gaussianity.

Table 2: Weighted Mean Results for 43 Redshift Measurements, where the unit of  $H(z)$  is  $\text{km s}^{-1} \text{Mpc}^{-1}$ .

Bin	N	$z$	$H(z)$	$H(z)$ (1 $\sigma$ Range)	$H(z)$ (2 $\sigma$ Range)	$N_\sigma$
3 or 4 Measurements per Bin						
1	3	0.0895	68.9	59.4-78.5	49.9-88.0	1.98
2	4	0.1847	76.0	73.1-78.9	70.2-81.8	1.12
3	3	0.2412	79.6	77.0-82.2	74.4-84.8	1.56
4	4	0.3776	81.7	79.9-83.5	78.1-85.3	1.85
5	3	0.4095	83.8	76.9-90.7	70.0-97.6	0.61
6	3	0.4329	86.2	83.0-89.4	79.8-92.6	1.02
7	4	0.5086	90.0	88.1-91.9	86.2-93.8	0.98
8	4	0.6024	95.8	94.0-97.6	92.2-99.4	0.06
9	3	0.7201	96.6	91.8-101.4	87.0-106.2	0.71
10	4	0.9287	129.2	118.3-140.1	107.4-151.0	0.07
11	4	1.4301	158.3	149.4-167.2	140.5-176.1	0.05
12	2	1.8331	196.0	164.7-227.3	133.4-258.6	1.07
13	2	2.3487	223.7	218.4-229.0	213.1-234.3	0.88
4 or 5 Measurements per Bin						
1	5	0.1664	75.7	72.4-79.0	69.1-82.3	1.18
2	5	0.2321	78.6	76.3-80.9	74.0-83.2	1.55
3	4	0.3776	81.7	79.9-83.5	78.1-85.3	1.85
4	5	0.4276	85.4	82.4-88.4	79.4-91.4	1.26
5	5	0.5074	90.1	88.3-91.9	86.5-93.7	1.33
6	5	0.6061	95.6	93.8-97.4	92.0-99.2	0.23
7	5	0.7681	102.8	97.3-108.3	91.8-113.8	0.45
8	5	1.3647	157.5	149.3-165.7	141.1-173.9	0.32
9	2	1.8331	196.0	164.7-227.3	133.4-258.6	1.07
10	2	2.3487	223.7	218.4-229.0	213.1-234.3	0.88
5 or 6 Measurements per Bin						
1	5	0.1664	75.7	72.4-79.0	69.1-82.3	1.18
2	5	0.2321	78.6	76.3-80.9	74.0-83.2	1.55
3	6	0.3785	81.7	80.0-83.5	78.2-85.3	1.75
4	6	0.4276	85.7	82.8-88.6	79.9-91.5	1.89
5	5	0.5263	90.7	89.0-92.4	87.3-94.1	1.13
6	6	0.6312	97.5	95.6-99.4	93.7-101.3	0.51
7	6	1.3128	153.0	145.3-160.7	137.6-168.4	0.28
8	2	1.8331	196.0	164.7-227.3	133.4-258.6	1.07
9	2	2.3487	223.7	218.4-229.0	213.1-234.3	0.88
5, 6 or 7 Measurements per Bin						
1	7	0.1767	75.4	72.6-78.2	69.8-81.0	1.80
2	7	0.3333	81.1	79.6-82.6	78.1-84.1	2.27
3	7	0.4288	85.8	82.9-88.7	80.0-91.6	1.71
4	6	0.5247	90.4	88.8-92.0	87.1-93.7	0.89
5	7	0.6331	97.7	95.8-99.6	93.9-101.5	0.55
6	5	1.3647	157.5	149.3-165.7	141.1-173.9	0.32
7	2	1.8331	196.0	164.7-227.3	133.4-258.6	1.07
8	2	2.3487	223.7	218.4-229.0	213.1-234.3	0.88

Since the median statistics technique originally proposed by Gott et al.[53] has a prerequisite which assumes that measurements of a given quantity are independent and that there are no systematic effects, and as previously mentioned the correlative measurements of OHD from Blake et al. [38] and Alam et al. [42] may contaminate the results, we decide to remove these data for the sake of purity. Table 3 displays the results from median statistics technique. After assuming that there is no overall systematic error in the reduced OHD as a whole and all the remaining measurements are independent, it is convenient to use the median statistics to combine the OHD. As the number of the measurements increases and approaches to infinity, the median can be presented as a true value, therefore, this technique has the merits of reducing the effect of outliers of a set of measurements on the estimate of a true median value. Nevertheless, although OHD are a bit of short in quantity as opposed to the large amount of measurements needed to reveal the true value, we still employ this technique for comparison purpose. If  $N$  measurements are considered, the probability of finding the true median value between values  $N_i$  and  $N_{i+1}$  is [53]

$$P_i = \frac{2^{-N} N!}{i!(N-1)!}, \quad (9)$$

where  $i = 1, 2, \dots, N$ , and  $N!$  represents the factorial of  $N$ . After applying this technique to the reduced 37 OHD for binning, we obtain the binned results as listed in Table 3, applying the same binning scheme presented above. The results seem reasonable, but the precision is less than the weighted mean results, which may be caused by the less amount of OHD.

Even though the OHD obtained from BAO method are model-independent, one can still be confused by the employed fiducial models. Therefore, to avoid the confusion and also for comparison purpose, we decide to exclude the OHD from BAO method and only consider the cosmic chronometer case, which also have the merit of being independent with each other. Table 4 and 5 present the results from both binning methods. The results are all reasonable as well, and compared to the full binned OHD, the discrepancies are considerably small, which can be the evidence of the validity of the OHD derived from BAO method. Since the different measurements per bin does not significantly affect the results, we can acknowledge the robustness of the binning methods.

#### 4 Testing the $\Lambda$ CDM model with $Omh^2(z_2; z_1)$ diagnostic

In our analysis, the validity of  $Omh^2(z_2; z_1)$  diagnostic can be tested using  $H(z)$  results from cosmological independent measurements. On the basis of the above section, we apply binned OHD from both the weighted mean technique and

Table 3: Median Statistics Results for 37 reduced Redshift Measurements, where the unit of  $H(z)$  is  $\text{km s}^{-1} \text{Mpc}^{-1}$ .

Bin	N	$z$	$H(z)$	$H(z)$ (1 $\sigma$ Range)	$H(z)$ (2 $\sigma$ Range)
3 or 4 Measurements per Bin					
1	3	0.09	69.0	49.3-88.7	29.6-108.4
2	4	0.189	75.0	68.5-81.5	62.0-88.0
3	3	0.27	79.7	65.7-93.7	51.7-107.7
4	3	0.352	83.0	69.5-96.5	56-110.0
5	4	0.4125	86.8	76.1-97.5	65.4-108.2
6	4	0.474	90.9	53.5-128.4	16.0-165.8
7	4	0.6365	98.2	88.2-108.2	78.2-118.2
8	4	0.89	121.0	99.5-142.5	78.0-164.0
9	4	1.3965	164.0	146.5-181.5	129.0-199.0
10	4	2.1525	212.0	188.0-236.0	164.0-260.0
4 or 5 Measurements per Bin					
1	5	0.12	69.0	57.0-81.0	45.0-93.0
2	5	0.24	77.0	63.0-91.0	49.0-105.0
3	5	0.3802	83.0	69.5-96.5	56.0-110.0
4	5	0.4497	87.1	75.9-98.3	64.7-109.5
5	5	0.593	97.0	85.0-109.0	73.0-121.0
6	4	0.89	121.0	99.5-142.5	78.0-164.0
7	4	1.3965	164.0	146.5-181.5	129.0-199.0
8	4	2.1525	212.0	188.0-236.0	164.0-260.0
4, 5 or 6 Measurements per Bin					
1	5	0.12	69.0	57.0-81.0	45.0-93.0
2	5	0.24	77.0	63.0-91.0	49.0-105.0
3	5	0.3802	83.0	69.5-96.5	56.0-110.0
4	6	0.4598	88.1	76.0-100.2	63.9-112.3
5	6	0.7305	98.2	85.7-110.7	73.2-123.2
6	6	1.3315	157.0	138.0-176.0	119.0-195.0
7	4	2.1525	212.0	188.0-236.0	164.0-260.0
4, 6 or 7 Measurements per Bin					
1	7	0.17	72.9	60.9-84.9	48.9-96.9
2	6	0.315	83.0	69.3-96.8	55.5-110.5
3	7	0.43	87.1	75.9-98.3	64.7-109.5
4	7	0.68	97.0	84.0-110.0	71.0-123.0
5	6	1.3315	157.0	138.0-176.0	119.0-195.0
6	4	2.1525	212.0	188.0-236.0	164.0-260.0

the median statistics technique to the two-point  $Omh^2(z_2; z_1)$  diagnostic.

If  $Om(z_2; z_1)$  is always a constant at any redshifts, then it demonstrates that the DE is of the cosmological constant nature. In order to compare directly with the results from CMB, Sahni et al. [54] introduced a more convenient expression of the two-point diagnostic, i.e.,

$$Omh^2(z_2; z_1) = \frac{h^2(z_2) - h^2(z_1)}{(1+z_2)^3 - (1+z_1)^3}, \quad (10)$$

where  $h(z) = H(z)/100 \text{ km s}^{-1} \text{Mpc}^{-1}$ . The binned  $H(z)$  points calculated based upon the aforementioned binning methods in each case therefore yields  $N(N-1)/2$  model-independent measurements of the  $Omh^2(z_2; z_1)$  diagnostic, as shown in Figs. 2-7, where the uncertainty  $\sigma_{Omh^2(z_2; z_1)}$  can

Table 4: Weighted Mean Results for Method I Measurements, where the unit of  $H(z)$  is  $\text{km s}^{-1} \text{Mpc}^{-1}$ .

Bin	N	$z$	$H(z)$	$H(z)$ (1 $\sigma$ Range)	$H(z)$ (2 $\sigma$ Range)	$N_\sigma$
3 or 4 Measurements per Bin						
1	3	0.0895	68.9	59.4-78.5	49.9-88.0	1.98
2	4	0.1847	76.0	73.1-78.9	70.2-81.8	1.12
3	3	0.3089	80.6	71.0-91.2	61.5-99.7	1.46
4	4	0.4035	83.6	77.5-89.7	71.3-95.9	1.06
5	4	0.4691	85.0	77.7-92.3	70.4-99.6	1.34
6	3	0.6866	97.7	91.7-103.6	85.8-109.5	0.51
7	3	0.8834	118.8	105.9-131.7	93.0-144.6	0.85
8	4	1.2798	166.6	156.6-176.6	146.6-186.6	1.20
9	3	1.58	149.3	136.5-162.1	123.7-174.9	0.33
3, 4 or 5 Measurements per Bin						
1	5	0.1664	75.7	72.4-79.0	69.1-82.3	1.18
2	5	0.2221	76.1	71.7-80.5	67.3-84.9	1.90
3	5	0.412	85.3	79.8-90.8	74.2-96.4	1.17
4	5	0.5897	90.1	84.7-85.5	79.3-100.9	0.70
5	4	0.5074	111.4	102.6-120.2	93.8-129	0.86
8	4	1.2798	166.6	156.6-176.6	146.6-186.6	1.20
9	3	1.58	149.3	136.5-162.1	123.7-174.9	0.33
5 or 6 Measurements per Bin						
1	5	0.1664	75.7	72.4-79.0	69.1-82.3	1.18
2	5	0.2221	76.1	71.7-80.5	67.3-84.9	1.90
3	5	0.412	85.3	79.8-90.8	74.2-96.4	1.17
4	5	0.5897	90.1	84.7-85.5	79.3-100.9	0.70
5	5	0.8622	118.3	110.2-126.4	102.2-134.4	0.36
6	6	0.6312	161.1	152.5-169.7	143.9-178.3	0.16
3 or 4 Measurements per Bin						
1	3	0.09	69.0	49.3-88.7	29.6-108.4	
2	4	0.189	75.0	68.5-81.5	62.0-88.0	
3	3	0.28	83.0	69.0-97.0	55.0-111.0	
4	4	0.4002	85.1	72.7-97.4	60.4-109.8	
5	4	0.4741	90.9	53.5-128.4	16.0-165.8	
6	3	0.68	104.0	92.0-116.0	80.0-128.0	
7	3	0.88	117.0	94.0-140.0	71.0-163.0	
8	4	1.3315	164.0	145.0-183.0	126.0-202.0	
9	3	1.75	186.5	146.5-226.5	106.5-266.5	
3, 4 or 5 Measurements per Bin						
1	5	0.12	69.0	57.0-81.0	45.0-93.0	
2	5	0.27	77.0	63.0-91.0	49.0-105.0	
3	5	0.4004	87.1	74.2-100.0	61.3-112.9	
4	5	0.48	92.0	79.0-105.0	66.0-118.0	
5	4	0.8775	111.0	91.0-131.0	71.0-151.0	
6	4	1.3315	164.0	145.0-183.0	126.0-202.0	
7	3	1.75	172.5	146.5-226.5	106.5-266.5	
5 or 6 Measurements per Bin						
1	5	0.12	69.0	57.0-81.0	45.0-93.0	
2	5	0.27	77.0	63.0-91.0	49.0-105.0	
3	5	0.4004	87.1	74.2-100.0	61.3-112.9	
4	5	0.48	92.0	79.0-105.0	66.0-118.0	
5	5	0.88	117.0	97.0-137.0	77.0-157.0	
6	6	1.48	172.5	146.7-198.3	120.9-224.1	

be expressed as follows,

$$\sigma_{\text{Omh}^2(z_2; z_1)}^2 = \frac{4 \left( h^2(z_2) \sigma_{h(z_2)}^2 + h^2(z_1) \sigma_{h(z_1)}^2 \right)}{\left( (1+z_2)^3 - (1+z_1)^3 \right)^2}. \quad (11)$$

For  $\Lambda$ CDM, we have  $\text{Omh}^2 \equiv \Omega_m h^2$ . The value of  $\Omega_m h^2$  is constrained tightly by the Planck observations to be centered around 0.14 for the base of  $\Lambda$ CDM model fit [9]: the Planck temperature power spectrum data alone gives  $0.1426 \pm 0.0020$ , the Planck temperature data with lensing reconstruction gives  $0.1415 \pm 0.0019$ , and the Planck temperature data with lensing and external data gives  $0.1413 \pm 0.0011$ , all at  $1\sigma$  confidence level (CL). As stated in [9], we conservatively select  $0.1415 \pm 0.0019$  as the Planck value. If the  $\Lambda$ CDM model can hold, we would expect a constant value of  $\text{Omh}^2$  at any redshift intervals. Sahni et al. [54] compared their results with the Planck value to check the validity of the  $\Lambda$ CDM model. From our perspective, we should not follow their goals to test the tension between our results and the Planck value. Instead, we should first consider whether the values of  $\text{Omh}^2$  are constant or not. Here we only use the Planck value for comparison purpose.

As shown in Fig. 2, the results from the weighted mean cases, within  $1\sigma$  confidence region, are mostly consistent with both being constant (on average) and the Planck value, although some exceptions are presented and the best-fit  $\text{Omh}^2(\Delta z)$  values are fluctuated. Also, as shown in Fig. 3, the results from the median statistic cases are all consistent with both being constant and the Planck value within  $1\sigma$  confidence region. Note that these results are not continuous redshift intervals, it only shows the differences for different  $\Delta z$ . Therefore, it would be useful if we plot the consistent results alone to extrapolate the outcomes. Then we illustrate these results with the binned OHD from both binning methods in Figs. 4, which shows that the values of  $\text{Omh}^2$  for both binning methods fluctuate as the consistent redshift intervals change. The difference between the results from the weighted mean binning data and results from mean statistics is that the fluctuations from former situation are more intense which makes the tendency more distinct from the first four panels of Fig. 4. Thus, it is fair to come up with the conclusion that the validity of  $\Lambda$ CDM model is preserved.

Also, after binning the OHD from cosmic chronometer method, the corresponding  $\text{Omh}^2$  results with both binning techniques are demonstrated in Figs. 5-7. It is evident that the fluctuations of the best-fit  $\text{Omh}^2$  values are more intense than the results from full binned OHD for both binning methods. However, in average, the results are constant at  $1\sigma$  region. Hence, due to the two-point  $\text{Omh}^2(z_2; z_1)$  diagnostic combined with binned OHD results, the  $\Lambda$ CDM model is favored. However, we note that the error bars of these results are much bigger than the Planck result, therefore we can only conclude that the flat  $\Lambda$ CDM model cannot be ruled out.

## 5 Conclusions and Discussions

In this paper, motivated by the investigations on the nature of DE, we test the validity of  $\Lambda$ CDM with the two-point  $\text{Omh}^2(z_2; z_1)$  diagnostic by using 43 observational  $H(z)$  data (OHD) which are obtained from cosmic chronometer and BAO methods.

Firstly, instead of direct employment of the OHD on the  $\text{Omh}^2(z_2; z_1)$  diagnostic, we introduce the two binning methods: the weighted mean and median statistics to reduce the noise in the data. After binning OHD, we conclude that the original OHD are not inconsistent with Gassianity, and the binned data are all reasonable as Tables 2 and 3 displayed. The OHD derived from BAO method are not generally considered to be completely model-independent, even though as mentioned above the fiducial models indeed can not affect the results (e.g., see Alam et al. [42] P. 5), which means the data are model-independent after all. Nevertheless, due to the trust issue raised by some scientists, we also apply the binning method to the OHD derived from cosmic chronometer method alone as listed in Tables 4 and 5 for comparison. The results all seem reasonable and, compared to the full binned OHD, the discrepancies are considerably small, which can be the lateral evidence for the validity of the OHD derived from BAO method. Since the different measurements per bin does not significantly affect the results, we can acknowledge the robustness of the binning methods.

Secondly, combined with the set of binned OHD and, we exploit the  $\text{Omh}^2(z_2; z_1)$  diagnostic to test if the  $\text{Omh}^2$  values are being constant. From Figs. 2-7, we find that in average the  $\text{Omh}^2$  values are mostly being constant at  $1\sigma$  confidence region. Therefore, the flat  $\Lambda$ CDM model is not invalid. However, this does not mean that the dynamical DE models are not worth considering.

It is worth noticing that more independent OHD would bring more accuracy toward the binning methods, which can result in more reliable  $\text{Omh}^2(z_2; z_1)$  values. Also, as the number of OHD grows, the binned OHD would be more efficient as a data clarification instrument that can be employed on the cosmological constraints. The OHD with higher precision and larger amounts are in need and valuable.

**Acknowledgements** This work was supported by National Key R&D Program of China(2017YFA0402600), National Natural Science Foundation of China(Grants No. 11573006, 11528306)the Fundamental Research Funds for the Central Universities and the Special Program for Applied Research on Super Computation of the NSFC-Guangdong Joint Fund (the second phase).

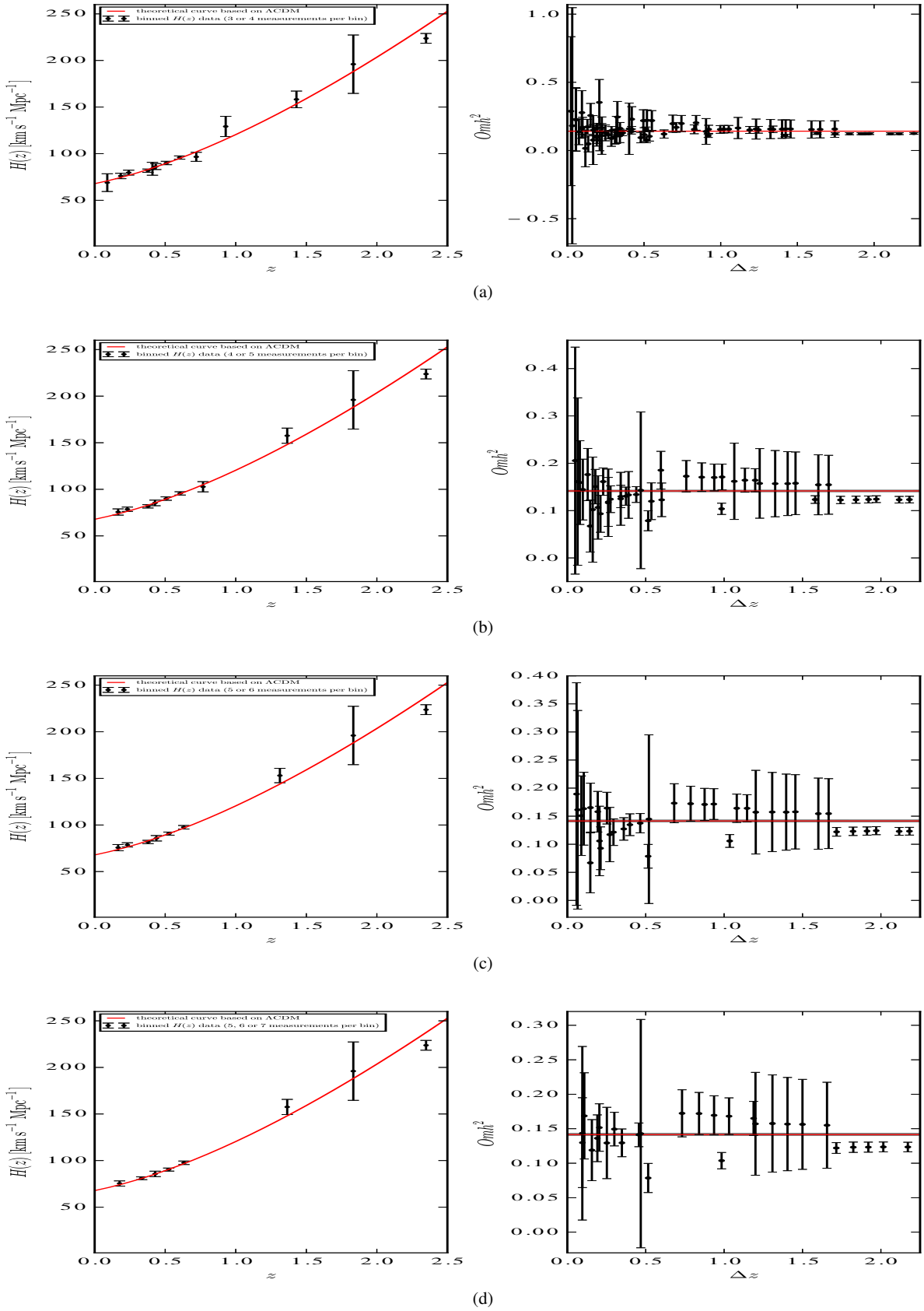


Fig. 2: Binned  $H(z)$  data based on full OHD and its corresponding  $Om h^2$  diagnostic values for the weighted mean technique. The panels (a), (b) (c) and (d) present the 3-4, 4-5, 5-6 and 5-6-7 measurements per bin case, respectively, where the red lines and gray shaded regions in the right panels represent the best-fit value of  $Om h^2$  and its uncertainties retrieved from the Planck CMB data.

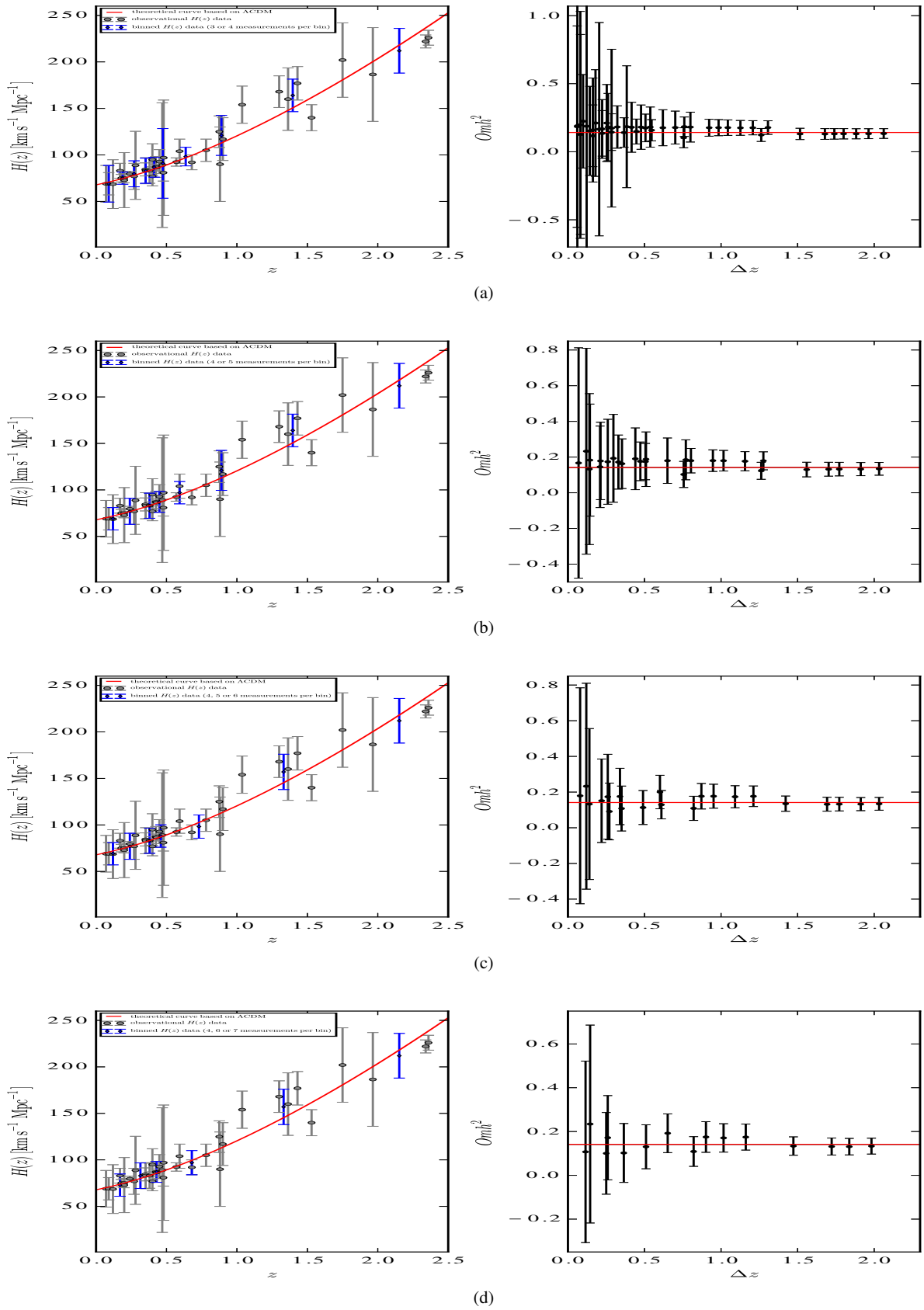


Fig. 3: 37 reduced OHD associated with binned data and its corresponding  $Om_{\text{h}}^2$  diagnostic values for the median statistics technique. The panels (a), (b) (c) and (d) present the 3-4, 4-5, 4-5-6 and 4-6-7 measurements per bin case, respectively, where the red lines in the right panels represent the best-fit value of  $Om_{\text{h}}^2$  retrieved from the Planck CMB data.

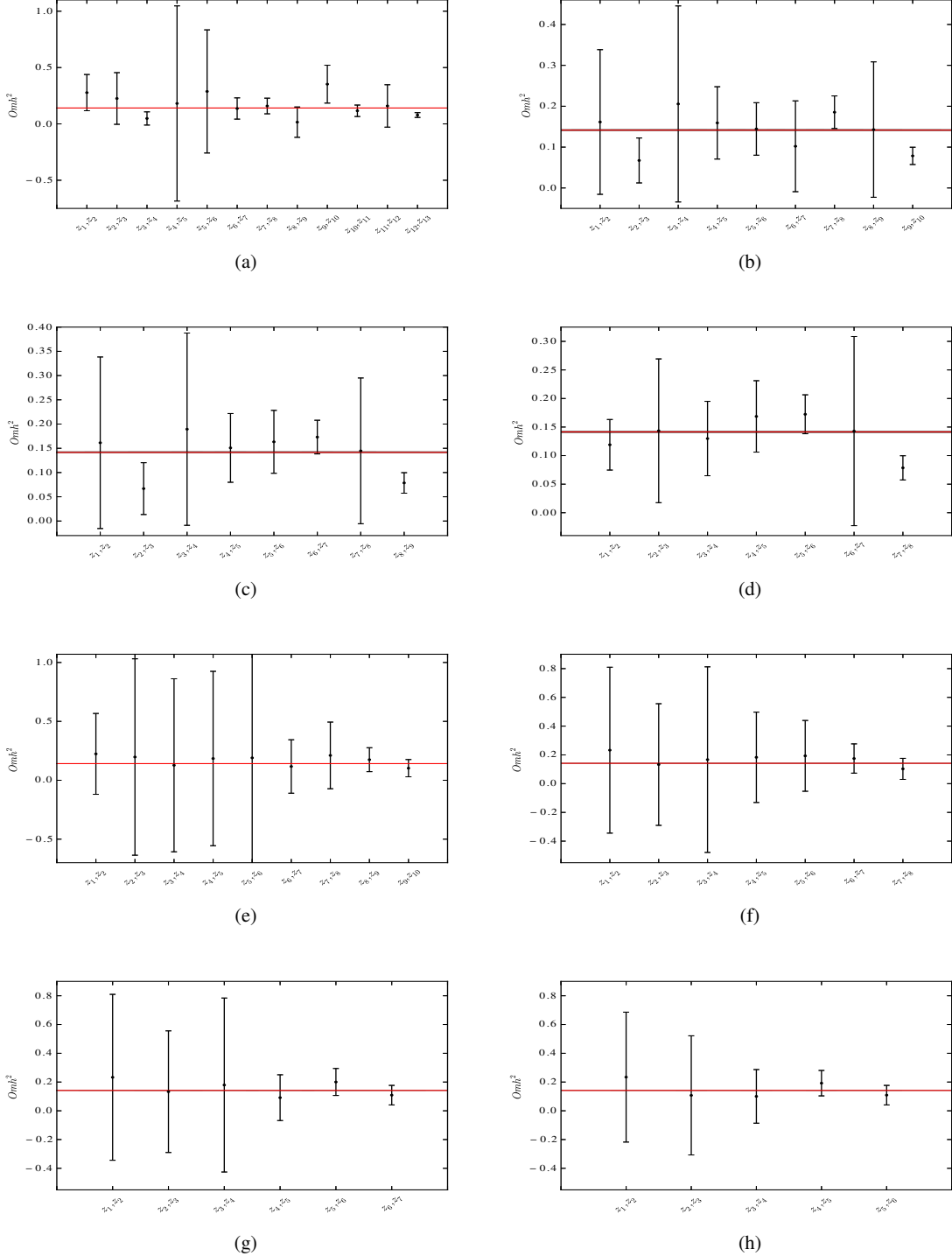


Fig. 4:  $Om h^2$  diagnostic values for both the weighted mean and median statistics techniques with respect to consistent redshifts. The panels (a), (b), (c) and (d) present the weighted mean 3-4, 4-5, 5-6, and 5-6-7 measurements per bin, respectively. The panels (e), (f) (g) and (h) present the median statistics 3-4, 4-5, 4-5-6 and 4-6-7 measurements per bin case, respectively, where the red lines represent the best-fit value of  $Om h^2$  retrieved from the Planck CMB data.

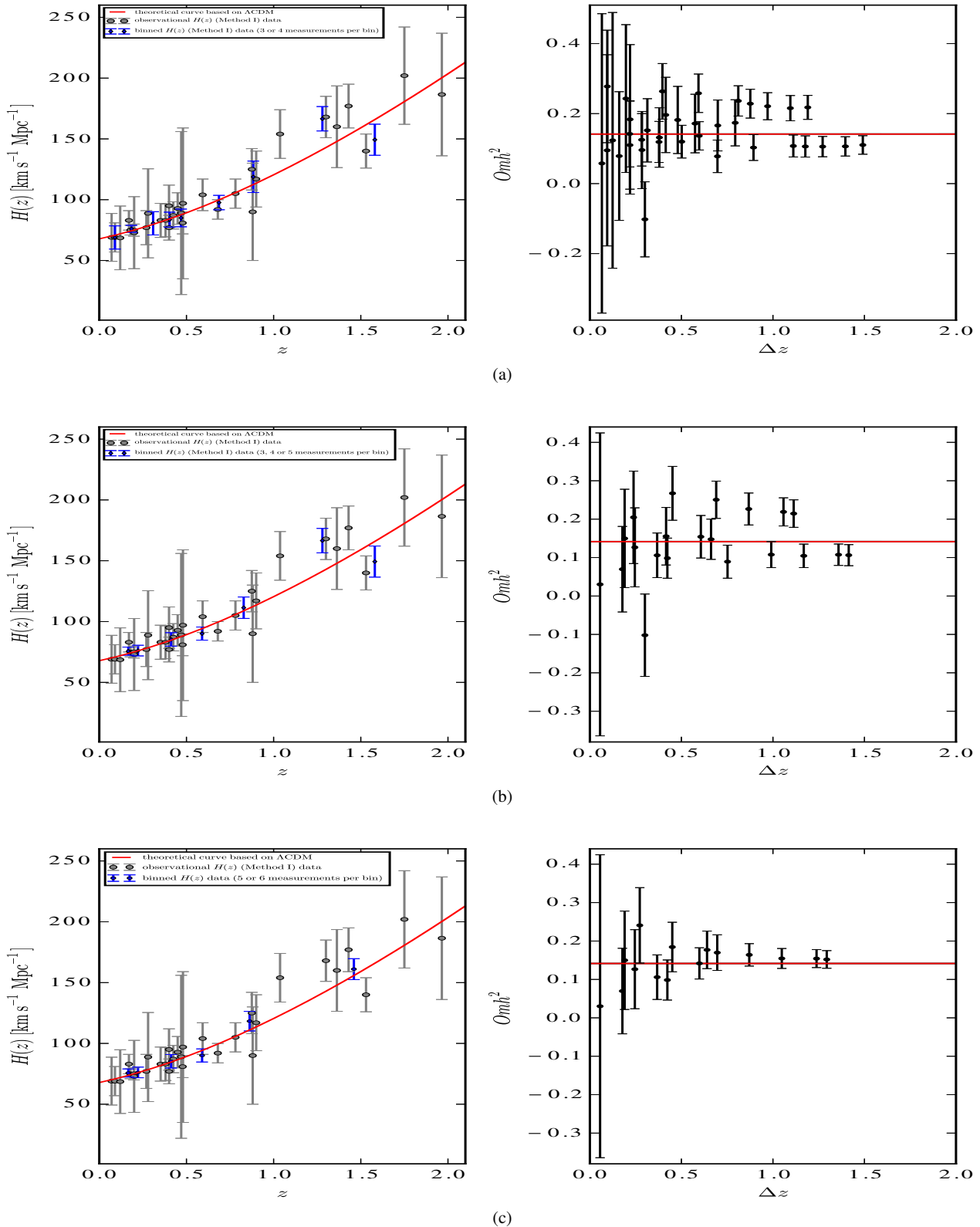


Fig. 5: OHD from cosmic chronometer method associated with binned data and its corresponding  $\Omega m h^2$  diagnostic values for the weighted mean technique. The panels (a), (b) and (c) present the 3-4, 3-4-5 and 5-6 measurements per bin case, respectively, where the red lines in the right panels represent the best-fit value of  $\Omega m h^2$  retrieved from the Planck CMB data.

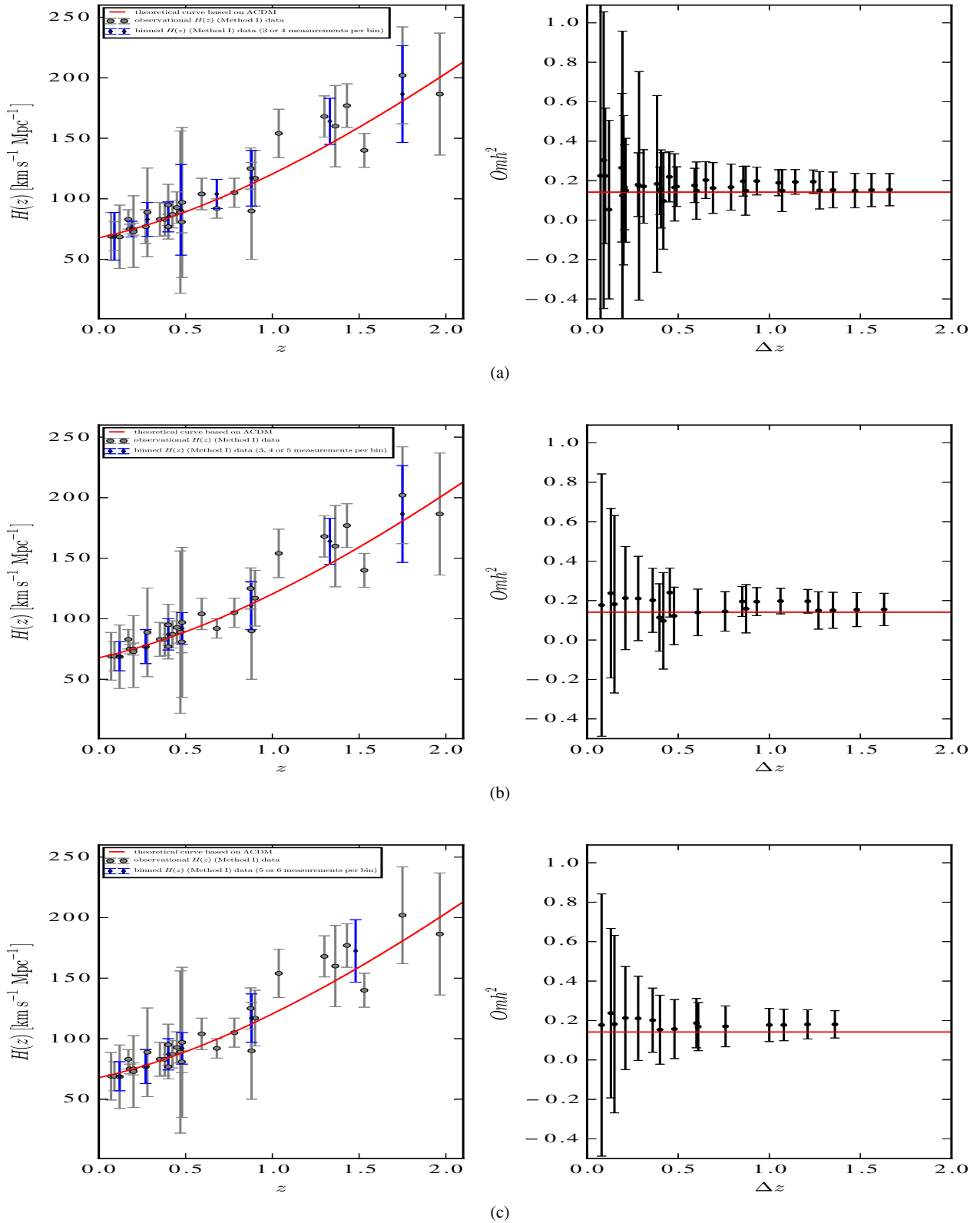


Fig. 6: Same as Fig. 5, but for the median statistics technique.

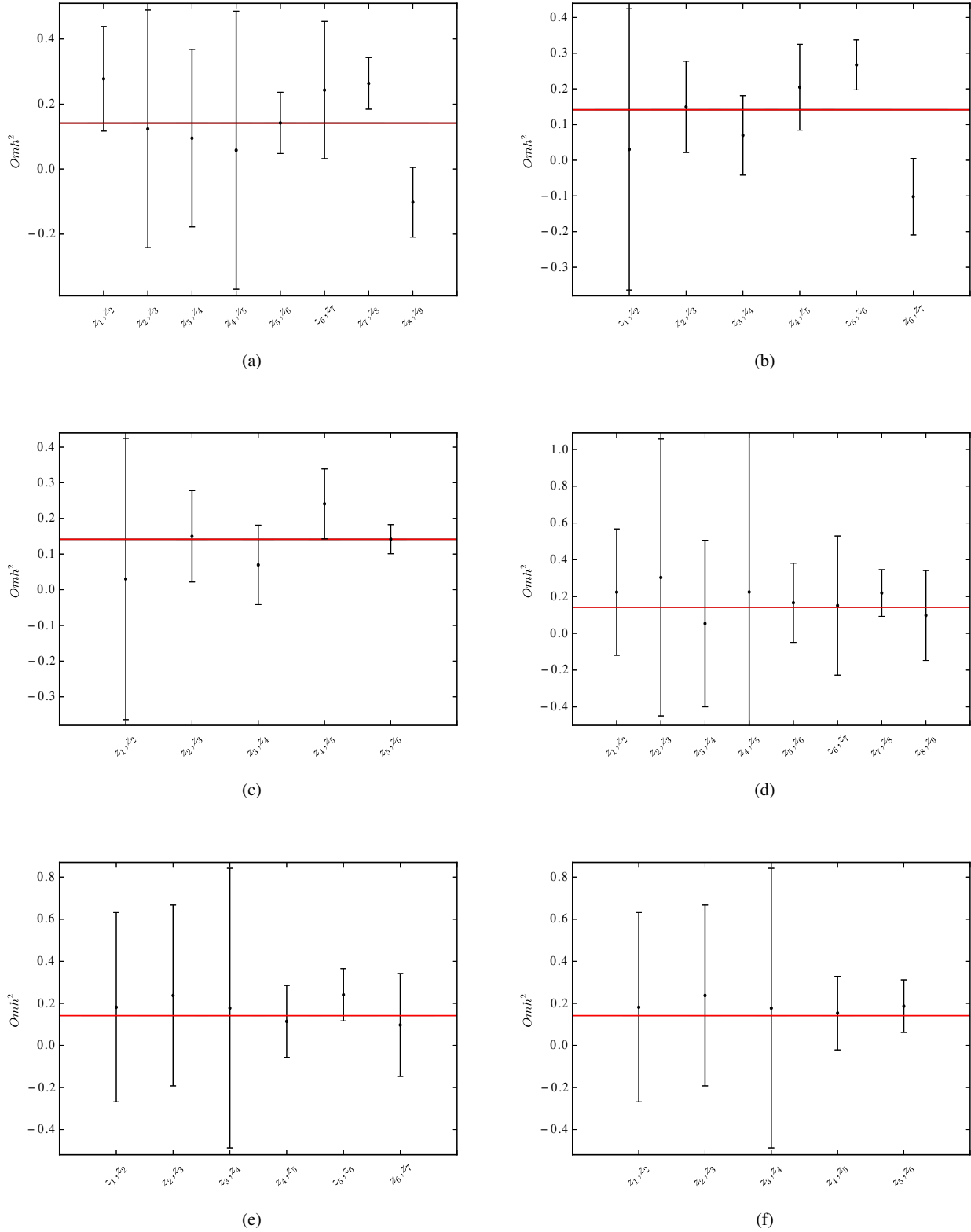


Fig. 7: Same as Fig. 4, but for OHD from cosmic chronometer method. The panels (a), (b) and (c) present the weighted mean 3-4, 3-4-5, and 5-6 measurements per bin, respectively, and the panels (d), (e) and (f) present the median statistics 3-4, 3-4-5, 5-6 measurements per bin, respectively, where the red lines in the panels represent the best-fit value of  $Om h^2$  retrieved from the Planck CMB data.

## References

1. J.A. Frieman, M.S. Turner, D. Huterer, Anne. Rev. Astron. Astr. **46**, 385 (2008). DOI 10.1146/annurev.astro.46.060407.145243
2. D.H. Weinberg, M.J. Mortonson, D.J. Eisenstein et al., Phys. Rep. **530**, 87 (2013). DOI 10.1016/j.physrep.2013.05.001
3. A.G. Riess, A.V. Filippenko, P. Challis et al., Astron. J. **116**, 1009 (1998). DOI 10.1086/300499
4. S. Perlmutter, G. Aldering, G. Goldhaber et al., Astrophys. J. **517**, 565 (1999). DOI 10.1086/307221
5. N. Suzuki, D. Rubin, C. Lidman et al., Astrophys. J. **746**, 85 (2012). DOI 10.1088/0004-637X/746/1/85
6. D.J. Eisenstein, I. Zehavi, D.W. Hogg et al., Astrophys. J. **633**, 560 (2005). DOI 10.1086/466512
7. M. Kilbinger, L. Fu, C. Heymans et al., Mon. Not. R. Astron. Soc. **430**, 2200 (2013). DOI 10.1093/mnras/stt041
8. B.A. Benson, T. de Haan, J.P. Dudley et al., Astrophys. J. **763**, 147 (2013). DOI 10.1088/0004-637X/763/2/147
9. Planck Collaboration, P.A.R. Ade, N. Aghanim et al., Astron. Astrophys. **594**, A13 (2016). DOI 10.1051/0004-6361/201525830
10. S. Dodelson, V.K. Narayanan, M. Tegmark et al., Astrophys. J. **572**, 140 (2002). DOI 10.1086/340225
11. W.L. Freedman, B.F. Madore, V. Scowcroft et al., Astrophys. J. **758**, 24 (2012). DOI 10.1088/0004-637X/758/1/24
12. M. Li, X.D. Li, S. Wang et al., Communications in Theoretical Physics **56**, 525 (2011). DOI 10.1088/0253-6102/56/3/24
13. S. Weinberg, Rev. Mod. Phys. **61**, 1 (1989). DOI 10.1103/RevModPhys.61.1
14. I. Zlatev, L. Wang, P.J. Steinhardt, Phys. Rev. Lett. **82**, 896 (1999). DOI 10.1103/PhysRevLett.82.896
15. G.B. Zhao, M. Raveri, L. Pogosian et al., Nature Astronomy **1**, 627 (2017). DOI 10.1038/s41550-017-0216-z
16. B. Ratra, P.J.E. Peebles, Phys. Rev. D **37**, 3406 (1988). DOI 10.1103/PhysRevD.37.3406
17. C. Wetterich, Nucl. Phys. B **302**, 668 (1988). DOI 10.1016/0550-3213(88)90193-9
18. R.R. Caldwell, Phys. Lett. B **545**, 23 (2002). DOI 10.1016/S0370-2693(02)02589-3
19. C. Armendariz-Picon, V. Mukhanov, P.J. Steinhardt, Phys. Rev. Lett. **85**, 4438 (2000). DOI 10.1103/PhysRevLett.85.4438
20. C. Armendariz-Picon, V. Mukhanov, P.J. Steinhardt, Phys. Rev. D **63**(10), 103510 (2001). DOI 10.1103/PhysRevD.63.103510
21. B. Feng, X. Wang, X. Zhang, Phys. Lett. B **607**, 35 (2005). DOI 10.1016/j.physletb.2004.12.071
22. B. Feng, M. Li, Y.S. Piao et al., Phys. Lett. B **634**, 101 (2006). DOI 10.1016/j.physletb.2006.01.066
23. V. Sahni, A. Shafieloo, A.A. Starobinsky, Phys. Rev. D **78**(10), 103502 (2008). DOI 10.1103/PhysRevD.78.103502
24. C. Zunckel, C. Clarkson, Phys. Rev. Lett. **101**(18), 181301 (2008). DOI 10.1103/PhysRevLett.101.181301
25. A. Shafieloo, V. Sahni, A.A. Starobinsky, Phys. Rev. D **86**(10), 103527 (2012). DOI 10.1103/PhysRevD.86.103527
26. T.J. Zhang, C. Ma, T. Lan, Adv. Astron. **2010**, 184284 (2010). DOI 10.1155/2010/184284
27. L. Yang, H.Y. Wan, T.J. Zhang, T. Yanke, ArXiv e-prints (2017)
28. R. Jimenez, A. Loeb, Astrophys. J. **573**, 37 (2002). DOI 10.1086/340549
29. R. Jimenez, L. Verde, T. Treu et al., Astrophys. J. **593**, 622 (2003). DOI 10.1086/376595
30. J. Simon, L. Verde, R. Jimenez, Phys. Rev. D **71**(12), 123001 (2005). DOI 10.1103/PhysRevD.71.123001
31. D. Stern, R. Jimenez, L. Verde et al., J. COSMOL. ASTROPART. P. **2**, 008 (2010). DOI 10.1088/1475-7516/2010/02/008
32. M. Moresco, A. Cimatti, R. Jimenez et al., J. COSMOL. ASTROPART. P. **8**, 006 (2012). DOI 10.1088/1475-7516/2012/08/006
33. C. Zhang, H. Zhang, S. Yuan et al., Res. Astron. Astrophys. **14**, 1221 (2014). DOI 10.1088/1674-4527/14/10/002
34. M. Moresco, Mon. Not. R. Astron. Soc. **450**, L16 (2015). DOI 10.1093/mnrasl/slv037
35. M. Moresco, L. Pozzetti, A. Cimatti et al., JCAP **5**, 014 (2016). DOI 10.1088/1475-7516/2016/05/014
36. A.L. Ratsimbazafy, S.I. Loubser, S.M. Crawford et al., Mon. Not. R. Astron. Soc. **467**, 3239 (2017). DOI 10.1093/mnras/stx301
37. E. Gaztañaga, A. Cabré, L. Hui, Mon. Not. R. Astron. Soc. **399**, 1663 (2009). DOI 10.1111/j.1365-2966.2009.15405.x
38. C. Blake, S. Brough, M. Colless et al., Mon. Not. R. Astron. Soc. **425**, 405 (2012). DOI 10.1111/j.1365-2966.2012.21473.x
39. L. Samushia, B.A. Reid, M. White et al., Mon. Not. R. Astron. Soc. **429**, 1514 (2013). DOI 10.1093/mnras/sts443
40. X. Xu, A.J. Cuesta, N. Padmanabhan et al., Mon. Not. R. Astron. Soc. **431**, 2834 (2013). DOI 10.1093/mnras/stt379
41. T. Delubac, J.E. Bautista, N.G. Busca et al., Asrton. Astrophys. **574**, A59 (2015). DOI 10.1051/0004-6361/201423969
42. S. Alam, M. Ata, S. Bailey et al., Mon. Not. R. Astron. Soc. **470**, 2617 (2017). DOI 10.1093/mnras/stx721

---

- 43. M. Moresco, F. Marulli, *Mon. Not. R. Astron. Soc.* **471**, L82 (2017). DOI 10.1093/mnrasl/slx112
- 44. O. Farooq, F. Ranjeet Madiyar, S. Crandall, B. Ratra, *Astrophys. J.* **835**, 26 (2017). DOI 10.3847/1538-4357/835/1/26
- 45. L. Samushia, B. Ratra, *Astrophys. J. Lett.* **650**, L5 (2006). DOI 10.1086/508662
- 46. V. Sahni, A. Starobinsky, *International Journal of Modern Physics D* **9**, 373 (2000). DOI 10.1142/S0218271800000542
- 47. S.M. Carroll, *Living Rev. Relativ.* **4**, 1 (2001). DOI 10.12942/lrr-2001-1
- 48. P.J. Peebles, B. Ratra, *Reviews of Modern Physics* **75**, 559 (2003). DOI 10.1103/RevModPhys.75.559
- 49. E.J. Copeland, M. Sami, S. Tsujikawa, *Int. J. Mod. Phys. D* **15**, 1753 (2006). DOI 10.1142/S021827180600942X
- 50. T. Clifton, P.G. Ferreira, A. Padilla et al., *Phys. Rep.* **513**, 1 (2012). DOI 10.1016/j.physrep.2012.01.001
- 51. O. Farooq, S. Crandall, B. Ratra, *Phys. Lett. B* **726**, 72 (2013). DOI 10.1016/j.physletb.2013.08.078
- 52. S. Podariu, T. Souradeep, J.R. Gott et al., III, *Astrophys. J.* **559**, 9 (2001). DOI 10.1086/322409
- 53. J.R. Gott, III, M.S. Vogeley, S. Podariu, B. Ratra, *Astrophys. J.* **549**, 1 (2001). DOI 10.1086/319055
- 54. V. Sahni, A. Shafieloo, A.A. Starobinsky, *Astrophys. J. Lett.* **793**, L40 (2014). DOI 10.1088/2041-8205/793/2/L40